**The Cryosphere
Discussions**

Ikaite crystals in melting sea ice – implications for pCO$_2$ and pH levels in Arctic surface waters

S. Rysgaard[1,2,3], R. N. Glud[3,4,5], K. Lennert[3], M. Cooper[2], N. Halden[2],
R. J. G. Leakey[4], F. C. Hawthorne[2], and D. Barber[1]

[1]Centre for Earth Observation Science, CHR Faculty of Environment Earth and Resources,
University of Manitoba, 499 Wallace Building, Winnipeg, MB R3T 2N2, Canada
[2]Department of Geological Sciences, CHR Faculty of Environment Earth and Resources,
University of Manitoba, 499 Wallace Building, Winnipeg, MB R3T 2N2, Canada
[3]Greenland Climate Research Centre, Greenland Institute of Natural Resources, Kivioq 2,
3900 Nuuk, Greenland
[4]Scottish Association for Marine Science, Scottish Marine Institute, Oban. PA37 1QA, UK
[5]Southern Danish University and NordCEE, Odense M, Denmark

Correspondence to: S. Rysgaard (rysgaard@cc.umanitoba.ca)

Discussion Paper | Discussion Paper | Discussion Paper | Discussion Paper

TCD

6, 1015–1035, 2012

Ikaite crystals in melting sea ice

S. Rysgaard et al.

Title Page

Abstract | Introduction

Conclusions | References

Tables | Figures

|◄ | ►|

◄ | ►

Back | Close

Full Screen / Esc

Printer-friendly Version

Interactive Discussion

Abstract

A major issue of Arctic marine science is to understand whether the Arctic Ocean is, or will be, a source or sink for air-sea CO_2 exchange. This has been complicated by the recent discoveries of ikaite ($CaCO_3 \cdot 6H_2O$) in Arctic and Antarctic sea ice, which
5   indicate that multiple chemical transformations occur in sea ice with a possible effect on CO_2 and pH conditions in surface waters. Here we report on biogeochemical conditions, microscopic examinations and x-ray diffraction analysis of single crystals from an actively melting 1.7 km^2 (0.5–1 m thick) drifting ice floe in the Fram Strait during summer. Our findings show that ikaite crystals are present throughout the sea ice but
10   with larger crystals appearing in the upper ice layers. Ikaite crystals placed at elevated temperatures gradually disintegrated into smaller crystallites and dissolved. During our field campaign in late June, melt reduced the ice flow thickness by ca. 0.2 m per week and resulted in an estimated 1.6 ppm decrease of pCO$_2$ in the ocean surface mixed layer. This corresponds to an air-sea CO_2 uptake of 11 mmol m^{-2} sea ice d^{-1} or to
15   3.5 ton km^{-2} ice floe week^{-1}.

1   Introduction

Recent work suggests that sea ice may play a central role in the control of the air-sea CO_2 flux in high latitude areas (Rysgaard et al., 2011). During winter, as sea ice grows, reduced air temperatures cause the brine volumes of surface sea ice to contract and
20   permeability to decrease, effectively stopping air-sea ice gas exchange (Loose et al., 2011). At the same time brine volume contraction further increases brine salinity, CO_2 concentration and supersaturation with respect to a suite of minerals, including several polymorphs of calcium carbonate ($CaCO_3$) (Assur, 1958). As CO_2 is rejected more efficiently than total alkalinity (TA) during ice formation (Rysgaard et al., 2007) this
25   will, over the winter, lead to enriched TA conditions relative to total dissolved inorganic carbon (TCO$_2$) conditions in sea ice as compared with the ratio in seawater. Recent

data from Antarctica also show enriched TA conditions in relation to TCO_2 conditions in sea ice (Fransson et al., 2011). The observation of TA:TCO_2 ratios as high as 2 indicate that calcium carbonate ($CaCO_3$) is formed in natural sea ice (Rysgaard et al., 2007, 2009]. Ikaite crystals ($CaCO_3 \cdot 6H_2O$) in sea ice have recently been discovered in both hemispheres (Dieckmann et al., 2008, 2010). Crystallization of $CaCO_3$ [Ca^{2+} + $2HCO_3^- \rightarrow CaCO_3(s) + H_2O + CO_2$] in the brine increases the concentration of CO_2 in the brine during growing sea ice conditions. The specific conditions promoting ikaite precipitation in sea ice are currently poorly understood, but if precipitation occurs in the porous bottom sea-ice layer, where the brine volume is larger than 5 % (Weeks and Ackley, 1986; Golden et al., 1998, 2007), the CO_2-enriched brine will exchange with seawater via gravity drainage (Notz and Worster, 2009). In contrast, the ikaite crystals could potentially remain trapped within the skeletal layer, where they will act as a store of TA, which will become a source of excess TA to the ocean water upon subsequent mineral dissolution when sea ice melts during summer (Rysgaard et al., 2007, 2009, 2011; Nedashkovsky et al., 2009). This will lower the $p\text{CO}_2$ of surface areas affected by melting sea ice and cause an increase in the air-sea CO_2 flux. More knowledge is, however, needed in order to understand carbonate crystal distribution in sea ice and their fate during summer melts. Here we report on biogeochemical conditions as well as microscopic examination and x-ray diffraction analysis on ikaite single crystals in an active melting 1.7 km^2 drifting ice floe passing through the Fram Strait in late June 2010.

2 Methods

The research was undertaken in summer 2010 as part of the ICE CHASER II research cruise on the UK icebreaker RRS *James Clark Ross* (JCR) (cruise JR219). The sampling location is presented in Fig. 1. On the 22 June, the JCR was anchored to a 1.7 km^2 drifting ice floe at 81° N, 5° E and drifted with the floe to 80° N, 2° E on 30 June 2010. The JCR was used as a laboratory for processing samples collected

Ikaite crystals in melting sea ice

S. Rysgaard et al.

Title Page

Abstract | Introduction

Conclusions | References

Tables | Figures

|◄ | ►|

◄ | ►

Back | Close

Full Screen / Esc

Printer-friendly Version

Interactive Discussion

on the ice flow. Sampling was performed ca. 0.5 km away from the ship and care was taken not to disturb the coring area that was only allowed to be reached from one side. Sea ice cores (9 cm diameter) were collected with a MARK II coring system (Kovacs Enterprises, Lebanon, NH) on three different sampling dates. We recognize that brine may be lost upon extraction of the core from the ice (Barber and Yackel, 1999). Thus, we may expect a brine loss of about 10 percent ($\pm 5\%$) from cores with brine volumes at levels considered here. However, brine loss from handling the ice core sections in the laboratory (see below) was minor as evaluated from the few droplets left in the polyethylene jars and on the clean sheets on which we worked. On each occasion, snow and sea ice thickness were recorded. Vertical temperature profiles were measured with a thermometer (Testo, Lemzkirch, Germany, and accuracy 0.1 °C) at 10-cm intervals in the snow and at the center of the cores through 3-mm holes drilled immediately after coring. Each sea ice core (one every sampling date) was then cut into 10-cm sections, and each section transferred to a 1-l polyethylene jar and kept cold (insulated thermo box) until further processing within an hour in the JCR laboratories. Water samples from 1 m below the sea ice were collected for salinity, temperature, TA and $T\text{CO}_2$ determinations with a glass syringe fitted with a gas tight Tygon tube inserted through the ice.

In the laboratory, sea ice density was determined by shaping the ice core section into well defined pieces with planar sides and then measuring the volume and weight of each piece. The pieces were then cut in two. One half was melted within 2 h and 25 ml collected for salinity measurements. The salinity of the melted sections (bulk salinity) was determined with a sonde (Knick Konductometer, Germany) calibrated to a PORTASAL salinometer. Brine volume in sea ice was calculated according to Cox and Weeks (1983) for temperatures below −2 °C, and according to Leppäranta and Manninen (1988) for temperatures within the range 0 °C to −2 °C. The rest of the meltwater was filtered through a GF/F filter for determination of chlorophyll a (Chl a) concentration. Chl a was extracted from filters for 24 h in 95 % buffered acetone and analyzed by high performance liquid chromatography (HPLC) (Mantoura et al., 1997).

Title Page

Abstract | Introduction

Conclusions | References

Tables | Figures

◄ | ►

◄ | ►

Back | Close

Full Screen / Esc

Printer-friendly Version

Interactive Discussion

The other half of each sea ice section was used to determine TA and TCO_2 concentrations in the following way: the ice segment was placed immediately in a gas-tight laminated (Nylon, ethylene vinyl alcohol, and polyethylene) plastic bag (Hansen et al., 2000) fitted with a 50-cm gas-tight Tygon tube and a valve for sampling. The weight of the bag containing the sea ice sample was recorded. Cold (1 °C) deionized water (25–50 ml) of known weight and TA and TCO_2 concentration was added together with 50 µl $HgCl_2$ (saturated solution). The plastic bag was then closed immediately and excess air and as much deionized water as possible quickly removed through the valve and weighed again. The weight of the deionized water accounted for 8–15 % of the sea ice weight. The sea ice was melted in the deionized water (at 0 °C), and the meltwater mixture transferred to a gas-tight vial (12 ml Exetainer, Labco High Wycombe, UK). Gas bubbles released from the melting sea ice were likewise transferred to gas-tight vials. In order to minimize gas exchange between brine and the ambient atmosphere, handling of each sea ice section took few minutes and a sea ice core could be processed within half an hour. Standard methods of analysis were used: TCO_2 concentrations were measured on a coulometer (Johnson et al., 1987), TA by potentiometric titration (Haraldsson et al., 1997), and CO_2 by gas chromatography. Routine analysis of Certified Reference Materials (provided by A. G. Dickson, Scripps Institution of Oceanography) verified that the accuracy of the TCO_2 and TA measurements was 0.5 µmol kg^{-1} and 2 µmol kg^{-1}, respectively. Bulk concentrations of TA and TCO_2 in the sea ice (C_i) were calculated as;

$$C_i = \frac{C_m W_m - C_a W_a}{W_i} \tag{1}$$

where C_m is the TA or TCO_2 concentration in the meltwater mixture, W_m the weight of the meltwater mixture, C_a the TA or TCO_2 concentration in the deionized water, W_a the weight of the artificial seawater, and W_i the weight of the sea ice.

Following the determination of TCO_2 and TA, the bulk partial pressure of CO_2 (pCO_2) and pH (on the total scale), were computed, using the temperature and salinity

conditions in the field and standard set of carbonate system equations, excluding nutrients, with the CO2SYS program of Lewis and Wallace (1998). We used the equilibrium constants of Mehrbach et al. (1973) refitted by Dickson and Millero (1987).

On 29 June, a sea ice core was collected for visualization and identification of $CaCO_3$ crystals in sea ice. The sea ice core was cut into 10 cm sections and transferred to 1-l polyethylene jars. The jars were transferred to a temperature controlled laboratory on board the JCR and each 10 cm section of sea ice cut into small pieces with a stainless steel knife and allowed to melt slowly over 12 h at −0.2 °C. The jars were then carefully swirled so crystals would concentrate at the bottom center of the jar. A portion of the crystals was then pipetted into a plankton counting chamber for microscopic examination at 100 and 200 magnification using a Zeiss (Carl Zeiss, Welwyn Garden City, UK) Axiovert S100 inverted microscope fitted with an AxioCam HRc digital camera and AvioVision version 4.7 image analysis software. Ten to fifteen images of crystals were obtained from each section. A dissolution experiment was performed on single crystals collected from the 0–10 cm section. Images of the crystals were obtained 80 times over 400 min while temperature was allowed to increase above 4 °C and the water droplet exposed to atmospheric air. The potential for loss of brine upon extraction from the sea ice will affect both rates and magnitudes of processes reported. We expect that in general our estimates will tend towards lower values over the expected range.

Sections of a parallel sea ice core (entire core) were kept at −18 °C and brought to the x-ray laboratory at the Department of Geological Sciences at the University of Manitoba. Here, sea ice was melted as described above and a small droplet of cold water containing transparent crystals deposited onto a cold glass slide resting on a chilled aluminum block containing a 1 cm central viewing hole. The crystals were first examined with a polarized light microscope to assess their optical properties and then mounted for x-ray study using a stereo binocular microscope. Selected crystals from 0–10 cm, 10–20 cm, 40–50 cm sections (distance from top of the sea ice) were dragged across the cold glass slide from the water droplet, using a metal probe, and

immersed into a drop of special purpose sampling oil, which restricted sublimation. Each crystal was then scooped up with a low x-ray scattering micro-loop and rapidly transferred to the nitrogen cold stream (−20 °C) on the x-ray diffraction instrument with a magnetic coupling goniometer head. The x-ray diffraction instrument consisted of a Bruker D8 three-circle diffractometer equipped with a rotating anode generator (Mo$K\alpha$ X-radiation), multi-layer optics, APEX-II CCD detector, and an Oxford 700 Series liquid-N Cryostream. The intensities of more than 100 reflections were harvested from six frame series (each spanning 15° in either ω or ϕ) collected to 60° 2θ using 0.6 s per 1° frame with a crystal-to-detector distance of 5 cm. In total 14 crystals were identified through successful indexing of observed x-ray diffraction maxima onto known characteristic unit cells. Of these 4 were ikaite and exhibited a distinct morphology as compared to other crystals identified as feldspar and quartz. The dimensions of 127 ikaite crystals, identified by light microscopy, were measured and the crystals grouped into size categories for describing the vertical size distribution through the ice.

3 Results

The average sea ice thickness at the sampling site, as determined from coring, decreased from 100 (±5) cm to 80 (±6) cm from 22 June to 29 June (2–3 cm d^{-1}) while the ice floe was drifting SSW. The decayed ice surface of 1–2 cm thickness on 22 June reduced to a mm thick layer during the 8 day sampling period. Air temperatures and water column temperatures 20 cm beneath the sea ice fluctuated around 0 °C (Table 1). Sea ice temperatures varied from 0 to −1.7 °C indicating a rapidly melting ice floe (Fig. 2). Bulk salinity over the study period varied from 0.2 to 6. The high temperatures and low salinities caused brine volume to be high. Average brine volumes during 22, 25 and 29 June were 0.16, 0.21 and 0.19, respectively. Brine volumes >0.05 indicate that the sea ice is permeable (Freitag and Eicken, 2003). No apparent trend with time was observed in the average TCO$_2$ and TA conditions. Concentrations of TCO$_2$ and TA in the vertical profiles (including dissolved ikaite) varied from 80 to 435 µmol kg^{-1}

melted sea ice and 210 to 680 $\mu mol\,kg^{-1}$ melted sea ice, respectively. The TA:TCO$_2$ ratio in sea ice was on all sampling dates significantly higher than in the water column (Tables 1 and 2). Chlorophyll a values in the sea ice ranged from 0.03 to 2.4 $\mu g\,kg^{-1}$ melted sea ice with highest concentration in the central part of the sea ice.

5   The crystals (10 to 1000 μm in size) observed in the sea ice were highly transparent with a rounded rhombic morphology (Fig. 3) and showed simple uniform extinction under crossed polarized light suggesting that they were well crystallized simple single crystals. All reflections fitted well to a monoclinic C-centered cell with $a = 8.806(2)$ $b = 8.315(2)$ $c = 11.027(2)$ Å $\beta = 110.571(12)$ $V = 755.9(4)$. From the general appear-
10   ance, optical properties and unit-cell determination, the crystals examined were ikaite (Hesse et al., 1983). Ikaite crystals were distributed throughout the sea ice with higher proportion of larger (>100 μm size) crystals in the surface layers of the ice (Fig. 4). One high quality crystal of ikaite, identified by single crystal x-ray diffraction, was allowed to decompose in a droplet of water at room temperature over 4 h (Fig. 5). This crystal lost
15   its transparency and gradually disaggregated into a multitude of smaller crystal components that resembled ikaite under the optical microscope. Of these, one tiny ($\sim$20 μm) fragment was harvested and examined by x-ray diffraction, and found to be ikaite as well. Other crystals identified from the sea ice were, quartz, feldspar, and corundum (crystals not shown).

20   **4   Discussion**

The sea ice floe melted rapidly during the investigation period as it drifted SSW in the Fram Strait. This was evident from both the ca. 20 cm week^{-1} decrease in thickness and from the freshening of bulk salinity and the very high brine volumes in the entire sea ice column. Much lower TA and TCO$_2$ concentrations in sea ice were measured
25   as compared to the underlying water (Tables 1 and 2). The TCO$_2$ concentration in the sea ice was ca. 10 % of the TCO$_2$ level in the underlying water and TA concentration in sea ice ca. 20 % of the TA in the water below. This, together with the higher TA:TCO$_2$

Title Page

Abstract | Introduction

Conclusions | References

Tables | Figures

|◄ | ►|

◄ | ►

Back | Close

Full Screen / Esc

Printer-friendly Version

Interactive Discussion

ratio of 1.83 to 2.12 in the sea ice as compared with the underlying water (1.09 to 1.12) suggests strongly the existence of carbonate crystals within the sea ice. Chl *a* and a diverse microbial community was also observed within the sea ice in several of our ice cores supporting previous findings of internal sea ice algal communities (Mock and Gradinger, 1999). This suggests that elevated brine volumes may facilitate internal algal growth due to advection of cells and nutrients from the sea ice-water interface.

Various ikaite crystal forms were isolated from the sea ice (Fig. 3). These ranged in size from 10 μm to large mm-size crystals. They were all highly transparent with a rounded rhombic morphology, and showed simple uniform extinction under crossed polarized light suggesting that they were all well-crystallized simple single crystals. Several of the crystals showed layered structures (Fig. 3) indicating historical growth patterns. Thus, it may be possible with the appropriate techniques to obtain a record of their formation and development. This will be an important task for future studies. The crystals identified by x-ray diffraction as ikaite had a morphology similar to the ones reported from Antarctica (Dieckmann et al., 2008) and from Arctic coastal fast ice locations in Svalbard (Dieckmann et al., 2010) and off Station Nord NE Greenland (Rysgaard et al., unpublished data). Furthermore, we observed ikaite crystals throughout the sea ice column with largest crystals in the upper layers of the sea ice in agreement with the observations from the other locations. Our results are made offshore in the Fram Strait within sea ice exiting the Arctic Ocean and thus, are a very strong suggestion that ikaite crystal within sea ice matrix may be representative for ice of the Arctic basin.

Normally ikaite crystals are considered stable at temperatures below 4 °C. At room temperature ikaite is unstable and decomposes into anhydrous calcium carbonate, vaterite and/or calcite and water (Marland, 1975; Shaikh, 1990; Mikkelsen et al., 1999). Furthermore, relative humidity has been identified as an important factor controlling the rate of decomposition of ikaite (Mikkelsen et al., 1999). The observation that a crystal of ikaite, identified by single crystal x-ray diffraction, disintegrated into smaller crystallites and eventually dissolved in a droplet of water exposed to atmospheric CO_2

at temperatures above 4 °C over a few hours (Fig. 5), confirms that ikaite crystals are highly unstable and will dissolve when temperature rises. Dissolving could in principle also be related to ikaite's reaction with CO_2 in the atmosphere changing the pH of the ikaite crystals' surroundings. More work is needed to resolve the kinetics of dissolving ikaite crystals. Melting of sea ice sections in gas tight bags at 0 °C also resulted in very low CO_2 levels in bulk sea ice sections throughout the ice column (Table 2). In addition, pH values increased to 10 in the bulk sections. It is likely that ikaite crystals in the lower parts of the sea ice will disintegrate before the ikaite crystals higher up in the sea ice as they will be in closer contact with the carbonate system of the underlying water due to higher brine volumes in these lower ice layers earlier in the melting season. This would explain why the largest crystals remained in the upper ice layers (Fig. 4). Another explanation for the largest ikaite crystals being found in the top layers of the sea ice is because they had the greatest opportunity (i.e. time) to grow into bigger crystals.

Melting of ice and dissolution of ikaite crystals will affect pCO_2 levels and the pH of surface water. We observed pCO_2 levels below sea ice of 157–210 µatm as compared with the 387 µatm in the atmosphere (Table 1). Furthermore, high pH values (pH = 8.3) were observed in surface waters. Thus, our findings support the conceptual model presented by Rysgaard et al. (2011). Here it was suggested that that sea-ice melt leads to stratification of the surface water column, and that mixing with melt water, already low in TCO_2 from melting ice, biological uptake and excess TA from the internal sea-ice $CaCO_3$ cycle, results in an increase in TA and a lowering of pCO_2 in the stratified surface waters. This would enhance the air-sea CO_2 flux.

Assuming that all ikaite crystals dissolve in the sea ice or in the mixed layer, melting of 0.2 m sea ice with the temperature, salinity, TA and TCO_2 conditions given in Table 2, into a 50 m thick mixed layer with water column characteristics as in Table 1, will result in a 1.6 ppm decrease in pCO_2 per week. It should be noted that the pCO_2 decrease would be many-fold higher in a thinner mixed layer, but the resultant air-sea CO_2 exchange would remain almost the same. Based on average conditions during the field campaign (Tables 1 and 2), this corresponds to an air-sea CO_2 uptake of

11 mmol m^{-2} sea ice d^{-1} or to 3.5 ton CO_2 km^{-2} ice floe week^{-1}. This is higher than the estimated primary production within the ice floe of 0.3–1.3 mmol m^{-2} sea ice d^{-1} (Glud et al., 2012) as assessed from >50 measurements of primary production incubations using the radio-14 carbon isotope. Thus, melting of sea ice and dissolution of ikaite crystals may potentially play a more important role for CO_2 uptake from the atmosphere during June, than sea ice algal primary productivity.

In the present study we melted sea ice at 0 °C to isolate ikaite crystals. However, we do not know if other carbonate crystals were present in the sea ice and dissolved by our melting procedure. Nor do we know if ikaite crystals are continuously formed and melted during the season; a process, which could greatly affect the air-sea CO_2 flux.

5 Conclusions

Our study shows that ikaite crystals were present throughout the ice column of a drifting sea ice floe in the Fram Strait. Larger crystals were observed in surface layers. Melting of the sea ice caused low pCO_2 conditions within sea ice (<1 µatm) and contributed to the low pCO_2 conditions in surface waters (157–210 µatm). In addition, pH in melting sea ice was high (pH = 9.9–10.1) and affected pH of surface waters (pH = 8.3–8.4). Melting of sea ice during June was estimated to be responsible for an air-sea CO_2 uptake of 11 mmol m^{-2} sea ice d^{-1}.

References

Assur, A.: Composition of sea ice and its tensile strength, in: Arctic Sea Ice, Vol. 598, 106–138, Natl. Res. Counc. Publ. Natl. Acad. Sci. Natl. Res. Counc., Washington, DC, 1958.

Barber, D. G. and Yackel, J.: The physical, radiative and microwave scattering characteristics of melt ponds on sea ice, Int. J. Remote Sens., 20, 2069–2090, 1999.

Cox, G. F. N. and Weeks W. F.: Equations for determining the gas and brine volumes in sea ice samples, J. Glaciol., 29, 306–316, 1983.

Dickson, A. G. and Millero F. J.: A comparison of the equilibrium constants for the dissociation of carbonic acid in seawater media, Deep-Sea Res., 34, 1733–1743, 1987.

Dickson, A. G. and Millero F. J.: Corrigenda, Deep-Sea Res., 36, p. 983, 1989.

Dieckmann, G. S., Nehrke, G., Papadimitriou, S., Göttlicher, J., Steininger, R., Kennedy, H., Wolf-Gladrow, D., and Thomas, D. N.: Calcium carbonate as ikaite crystals in Antarctic sea ice, Geophys. Res. Lett., 35, L08501, doi:10.1029/2008GL033540, 2008.

Dieckmann, G. S., Nehrke, G., Uhlig, C., Göttlicher, J., Gerland, S., Granskog, M. A., and Thomas, D. N.: Brief Communication: Ikaite ($CaCO_3 \cdot 6H_2O$) discovered in Arctic sea ice, The Cryosphere, 4, 227–230, doi:10.5194/tc-4-227-2010, 2010.

Fransson, A., Chierici, M., Yager, P. L., and Smith Jr., W. O.: Antarctic sea ice carbon dioxide system and controls, J. Geophys. Res., 116, C12035, doi:10.1029/2010JC006844, 2011.

Freitag, J. and Eicken, H.: Meltwater circulation and permeability of Arctic summer sea ice derived from hydrological field experiments, J. Glaciol., 49, 349–358, 2003.

Golden, K. M., Ackley, S. F., and Lytle, V. I.: The percolation phase transition in sea ice, Science, 282, 2238–2241, 1998.

Golden, K. M., Eicken, H., Heaton, A. L., Miner, J., Pringle, D. J., and Zhu, J.: Thermal evolution of permeability and microstructure in sea ice, Geophys. Res. Lett., 34, L16501, doi:10.1029/2007GL030447, 2007.

Hansen, J. W., Thamdrup, B., and Jørgensen, B. B.: Anoxic incubation of sediment in gas tight plastic bags: A method for biogeochemical process studies, Mar. Ecol. Prog. Ser., 208, 273–282, 2000.

Haraldsson, C., Anderson, L. G., Hasselöv, M., Hult, S., and Olsson, K.: Rapid, high-precision potentiometric titration of alkalinity in ocean and sediment pore water, Deep Sea Res. Pt. I, 44, 2031–2044, 1997.

Hesse, K. F., Kuppers, H., and Suess, E.: Refinement of the structure of Ikaite, $CaCO_3 \cdot 6H_2O$,

Full Screen / Esc

Printer-friendly Version

Interactive Discussion

Discussion Paper | Discussion Paper | Discussion Paper | Discussion Paper

Z. Krystallogr. Minera., 163, 227–231, 1983.

Johnson, K. M., Sieburth, J. M., Williams, P. J., and Brändström, L.: Coulometric total carbon dioxide analysis for marine studies: Automation and calibration, Mar. Chem., 21, 117–133, 1987.

Lampitt, R. S., Wishner, K. F., Turley, C. M., and Angel, M. V.: Marine snow studies in the Northeast Atlantic ocean: distribution, composition and role as a food source for migrating plankton, Mar. Biol., 116, 689–702, 1993.

Leppäranta, M. and Manninen, T.: The brine and gas content of sea ice with attention to low salinities and high temperatures, Internal Rep. 1988, 1–14, Finn. Inst. of Mar. Res., Helsinki, 1998.

Lewis, E. and Wallace D.: The program CO2SYS.EXE can be downloaded at: http://cdiac.esd.ornl.gov/oceans/co2rprtnbk.html, 1987.

Loose, B., Schlosser, P., Perovich, D., Ringelberg, D., Ho, D. T., and Takahashi, T., Richter-Menge, J., Reynolds, C. M., McGillis, W. R., and Tison, J-L.: Gas diffusion through columnar laboratory sea ice: implications for mixed-layer ventilation of CO_2 in the seasonal ice zone, Tellus, 63B, 23–39, 2011.

Mantoura, R. F. C., Barlow, R. G., and Head, E. J. H.: Simple isocratic HPLC methods for chlorophylls and their degradation products, in: Phytoplankton pigments in oceanography: guidelines to modern methods, edited by: Jeffrey, S. W., Mantoura, R. F. C., and Wright, S. W., UNESCO, Paris, 307–326, 1997.

Marland, G.: The stability of $CaCO_3.6H_2O$ (ikaite), Geochim. Cosmochim. Acta, 39, 83–91, 1975.

Mehrback, C., Culberson, H., Hawley, J. E., and Pytkowicz, R. M.: Measurement of the apparent dissociation constants of carbonic acid in seawater at atmospheric pressure, Limnol. Oceanogr., 18, 897–907, 1973.

Mikkelsen A, Andersen, A. B., Engelsen, S. B., Hansen, H. C., Larsen, O., and Skibsted, L. H.: Presence and dehydration of ikaite, calcium carbonate hexahydrate, in frozen shrimp shell, J. Agric. Food Chem., 47, 911–917, 1999.

Mock, T. and Gradinger, R.: Determination of Arctic ice algal production with a new in situ incubation technique, Mar. Ecol. Prog. Ser., 177, 15–26, 1999.

Nedashkovsky, A. P., Khvedynich, S. V., and Petovsky, T. V.: Alkalinity of sea ice in the high-latitudinal arctic according to the surveys performed at north pole drifting station 34 and characterization of the role of the arctic in the CO_2 exchange, Oceanology, 49, 55–63,

Ikaite crystals in melting sea ice

S. Rysgaard et al.

doi:10.1134/s000143700901007x, 2009.

Notz, D. and Worster, M. G.: Desalination processes of sea ice revisited, J. Geophys. Res., 114, C05006, doi:10.1029/2008JC004885, 2009.

Rysgaard, S., Glud, R. N., Sejr, M. K., Bendtsen, J., and Christensen, P. B.: Inorganic carbon transport during sea ice growth and decay: A carbon pump in polar seas, J. Geophys. Res., 112, C03016, doi:10.1029/2006jc003572, 2007.

Rysgaard, S., Bendtsen, J. B., Pedersen, L. T., Ramløv, H., and Glud, R. N.: Increased CO_2 uptake due to sea-ice growth and decay in the Nordic Seas, J. Geophys. Res., 114, C09011, doi:10.1029/2008JC005088, 2009.

Rysgaard, S., Bendtsen, J., Delille, B., Dieckmann, G., Glud, R. N., Kennedy, H., Mortensen, J., Papadimitriou, S., Thomas D. N., and Tison, J-L.: Sea ice contribution to air-sea CO_2 exchange in the Arctic and Southern Oceans, Tellus B, 63, 823–830, doi:10.1111/j.1600-0889.2011.00571.x, 2011.

Shaikh A. M.: A new crystal growth form of vaterite, $CaCO_3$, J. Appl. Cryst., 23, 263–265, 1990.

Weeks, W. F. and Ackley, S. F.: The growth, structure and properties of sea ice, in: The Geophysics of Sea Ice, edited by: Untersteiner, N., Plenum, New York, 1986.

Table 1. Surface water conditions (20 cm below sea ice) of temperature, salinity, TCO_2, TA and pCO_2 during the field campaign. Data from triplicate samples collected on three separate occasions are shown.

Date (2010)	TCO_2 μmol kg^{-1}	TA μmol kg^{-1}	TA:TCO_2	Temp. (°C)	Salinity	pH	pCO_2 (μatm)
25 June	1968.9	2201.5	1.12	−0.08	32.64	8.36	163
	1965.0	2196.9	1.12	−0.09	32.62	8.36	163
	1985.8	2197.6	1.11	−0.07	32.56	8.31	183
27 June	2005.9	2252.7	1.12	−0.49	33.27	8.38	157
	2010.8	2235.8	1.11	−0.04	32.59	8.33	176
	2016.2	2243.5	1.11	−0.70	32.64	8.35	169
29 June	1982.4	2173.2	1.10	−0.01	32.19	8.27	202
	1984.8	2168.9	1.09	−0.06	32.31	8.26	210
	1967.2	2160.8	1.10	−0.09	32.33	8.28	197

Table 2. Sea ice meltwater conditions of temperature, salinity, $T\text{CO}_2$, TA and $p\text{CO}_2$ during the field campaign. Values are mean ± standard deviation ($n = 10$) of vertical profile data from sea ice cores collected on the respective dates with $p\text{CO}_2$ conditions calculated at 0 dbar and 0 °C.

Date 2010	$T\text{CO}_2$ µmol kg^{-1}	TA µmol kg^{-1}	TA: $T\text{CO}_2$	Temp. (°C)	Salinity	pH (at 0 °C)	$p\text{CO}_2$ (µatm) (at 0 °C)
25 June	142.3 ± 23.9	304.4 ± 62.6	2.1	−1.3 ± 0.4	3.8 ± 1.3	10.1 ± 0.2	0.2 ± 0.1
27 June	229.0 ± 98.8	421.3 ± 126.1	1.8	−1.0 ± 0.5	4.2 ± 1.8	9.9 ± 0.3	0.5 ± 0.4
29 June	291.5 ± 116.5	533.0 ± 137.3	1.8	−1.1 ± 0.5	3.8 ± 1.8	10.1 ± 0.4	0.3 ± 0.5

Fig. 1. Map of the study area. The northern "X" marks the studied sea ice floe position on 22 June and the southern "X" marks its position on the 30 June 2010.
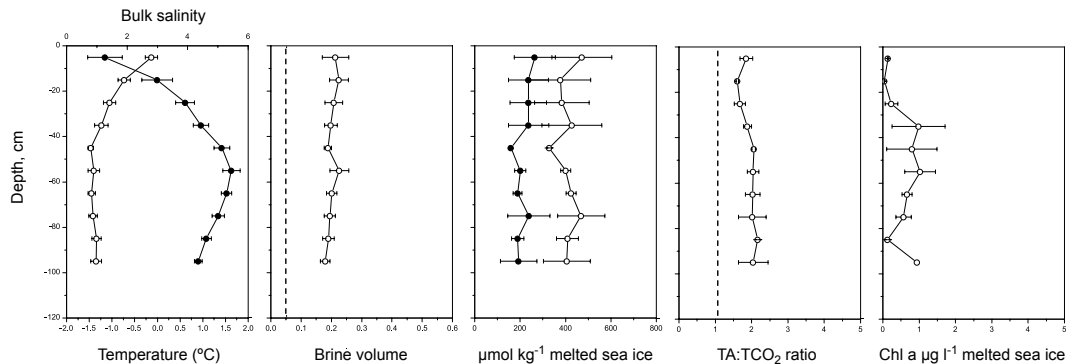
Fig. 2. Average conditions of temperature (-•-), bulk salinity (-○-), brine volumes, TA (-○-), $T\text{CO}_2$ (-•-), TA:$T\text{CO}_2$ ratio and Chl a at the coring site of the sea ice floe sampled during 22 to 30 June 2010. Values for temperature, salinity and brine volume are mean ± standard deviation ($n = 10$) and for TA, $T\text{CO}_2$, and Chl a ($n = 3$).
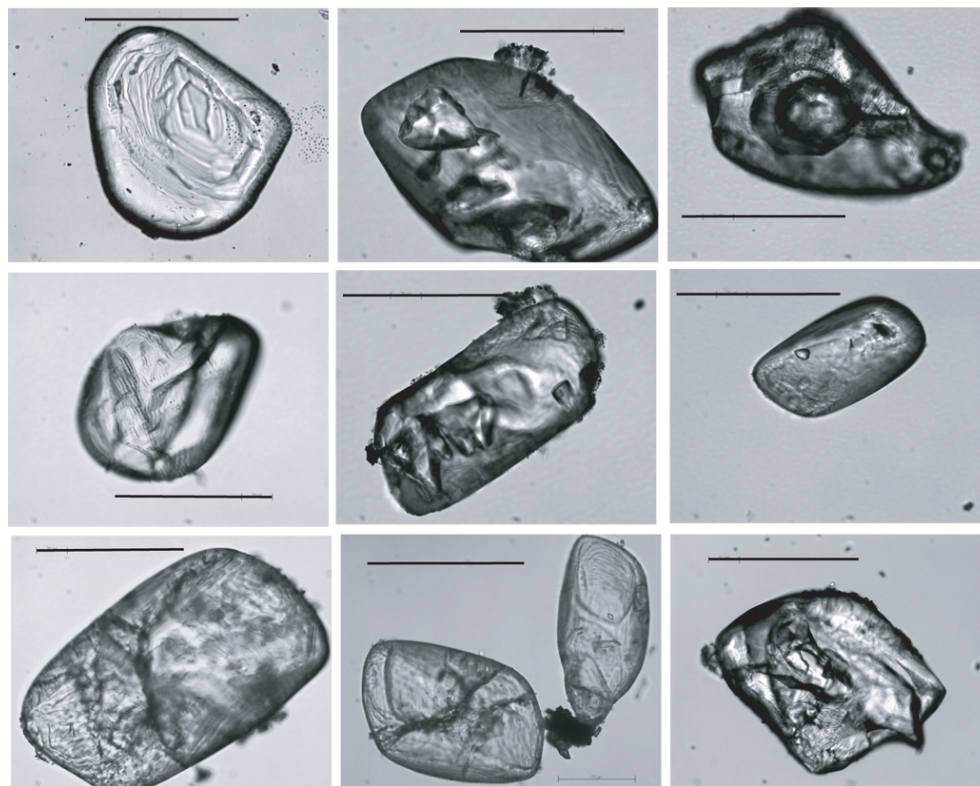
Fig. 3. Examples of ikaite crystals found in the sea ice. Scale bar is 100 μm.
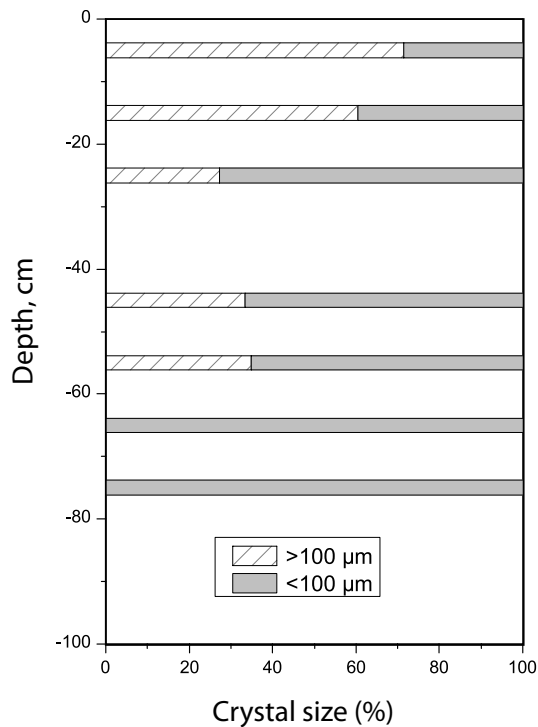
Fig. 4. Vertical distribution of small (<100 μm) and large (>100 μm) ikaite crystals in the sea ice.
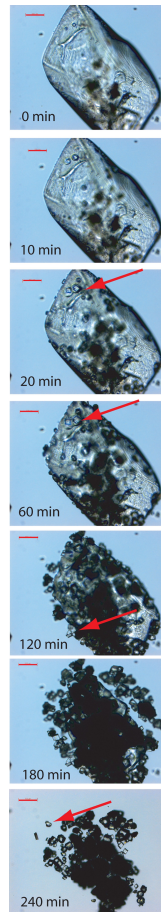
Fig. 5. Ikaite crystal dissolution during melting of sea ice over 240 min. Arrows point at smaller sub-units of crystals (also ikaite) that emerge during melting. Scale bar is 50 μm.